Characterization of micaceous minerals occurring in phosphate ores in Brazil: emphasis on the interstratified phyllosilicates

Juliana Angélica Evangelista Carvalho[1,2]
https://orcid.org/0000-0002-9285-9386

Paulo Roberto Gomes Brandao[1,3]
https://orcid.org/0000-0002-5893-1073

Andreia Bicalho Henriques[1,4]
https://orcid.org/0000-0001-5212-6527

[1]Universidade Federal de Minas Gerais – UFMG, Escola de Engenharia, Departamento de Engenharia de Minas, Belo Horizonte - Minas Gerais - Brasil.

E-mails: [2]juliana@demin.ufmg.br, labrx@demin.ufmg.br, [3]pbrandao@demin.ufmg.br, [4]abicalho@demin.ufmg.br, andreia@ufmg.br

Abstract

Micaceous minerals were characterized in three phosphatic ores from mines in Western Minas Gerais State, Brazil, all having complex chemical and mineralogical compositions, with emphasis on interstratified phyllosilicates. Knowledge of the relationship between the physical and chemical characteristics of the phyllosilicates contributed to a better understanding of the physicochemical processes in the mineral processing stages. Characterization of the minerals was carried out mainly by X-ray diffractometry (XRD), which allowed identifying vermiculite and three interstratified phyllosilicate phases. These minerals presented regular stratification of the unit cell, with different percentages of vermiculite and mica. Complementary studies by scanning electron microscopy (SEM) with EDS microanalysis, thermogravimetry and chemical analysis confirmed the identifications by XRD.

Keywords: interstratified phyllosilicates, vermiculite, mineralogy, phosphate ore.

1. Introduction

Phosphate ores are vital, non-renewable, non-recyclable and essential resources in the phosphorus-based chemical and fertilizer industry (Liu *et al.*, 2017). The main Brazilian phosphate deposits are located in the Alto do Paranaíba Igneous Province, in the states of Goiás (Catalão) and Minas Gerais (Araxá and Tapira) and have low P_2O_5 content (Albuquerque *et al.*, 2012). In these deposits, after the action of weathering, the micaceous apatitic ores can be encountered in the lower part of the isalteritic saprolite horizon, along with large amounts of goethite, anatase, quartz, phlogopite, vermiculite and interstratified phyllosilicates (Ażzone and Rubert, 2010).

Phyllosilicates are an important group of minerals that are part of the main components of the earth's crust. Minerals that have tetrahedral and octahedral layers or lamellae are phyllosilicates and are differentiated by the way the layers are stacked in the unit cell, such as: mica, chlorite, serpentine, clay minerals and vermiculite (Escamilla-Roa *et al.*, 2013; Bian and Kawi, 2020).

Phyllosilicate structures, in which two or more types of layers occur in a vertical stacking sequence, are described as the occurrence of mixed layers or interstratification (Reynolds, 1980; Plançon, 1981; Wang and Xu, 2006). Depending on the stacking order, interstratification can be considered as random, where there is no differentiable pattern in the sequence of layer types; ordered, where stacking is periodic; and partially ordered, which falls between the two extreme cases cited (Reynolds, 1980).

The most common ordering variety involves a regular alternation of two types of layers, and for some structures proper names exist. Randomly interstratified species are named according to the types of layers involved; therefore, the most abundant layer type is designated first as illite-smectite (Nadeau *et al.*, 1984; Veblen *et al.*, 1990), chlorite-talc (Schreyer *et al.*, 1982), smectite-illite (Reynolds, 1980; Veblen *et al.*, 1990), chlorite-smectite (Hillier, 1993), chlorite-serpentine (Bailey *et al.*, 1995; Xu and Veblen, 1996), talc-pyrophyllite (Reynolds, 1980), biotite-vermiculite (Gruner, 1934; Reynolds, 1980), mica-chlorite (Reynolds, 1980), mica-vermiculite (Reynolds, 1980), glauconite-smectite (Reynolds, 1980), kaolinite-smectite (Reynolds, 1980), chlorite-vermiculite (Reynolds, 1980) and chlorite-biotite (Xu *et al.*, 1996). For partially ordered species, there is still no consensus in literature regarding their names.

In currently mined phosphatic ores, apatite is the main phosphorus-bearing mineral and, therefore, the mineral of interest; while carbonate and silicate minerals, including phyllosilicates, quartz, clays, iron and titanium minerals, feldspars, pyroxenes, calcite and dolomite, are the main gangue minerals to be removed (Liu *et al.*, 2017; Sis and Chander, 2003; Mohammadkhani *et al.*, 2011).

The phyllosilicates are important gangue minerals and can pose serious problems in the selectivity in the froth flotation of these apatite ores. The weathered species, vermiculites and the

interstratified varieties, are particularly harmful (Assis *et al.*, 2010). The problem is even more serious for the interstratified silicates because they are poorly studied, mainly in the apatite ores. This is the main motivation of this study, to characterize these minerals and to understand their influence in the process.

This article's main objective is to identify the minerals present in three samples of micaceous apatite ores, with emphasis on interstratified phyllosilicates. The knowledge of the relationships between the physical and chemical characteristics of these phyllosilicates can contribute to a better understanding of the physical-chemical processes of the mineral processing of such ores. This study is justified in view of a near future scenario that points to the need to use these ores with more complex mineralogy.

2. Materials and methods

2.1 Sampling

The Mosaic sample was collected at Mosaic Fertilizantes in Araxá; the Rocha Alterada and Mica Base 1 samples were obtained from Yara Brasil Fertilizantes in Salitre. Both places are located in the western part of Minas Gerais State, Brazil.

The samples were dry comminuted in an agate mortar and sieved, obtaining 100% of particles passing the screen size of 38μm, which were used in the analyses for characterization.

2.2 Methods
2.2.1 Characterization

The mineral phases present in the samples were verified using the X-ray diffractometry (XRD) technique, powder method. The PW1710 X-ray diffractometer (Philips-PANalytical), with point detector, graphite crystal monochromator, copper tube (Z=29), average λ Kα = 1.54184Å and λ Kα1 = 1.54056Å was used. The instrument conditions were: power supply of 50kV and 35mA, scanning range from 3 to 90° in 2θ, step size of 0.06° (2θ) and counting time of 3 seconds.

When performing the XRD analyses, it was observed that misalignment may occur in the equipment's goniometer, thus displacing the peaks. This misalignment can even occur depending on how the sample is placed and adjusted to be analyzed in the equipment. Due to this potential problem, the following methodology was used: a natural sample of a chlorite schist, composed of chlorite, quartz and phlogopite called "linde" was used as standard to observe if there was displacement of the diffraction peaks during the analysis and make the necessary corrections.

This standard sample was submitted to quantitative analysis by X-ray diffractometry (XRD), using the procedure based in the Rietveld method.

The following procedure has always been followed: the standard was run in the diffractometer; then, the samples were analyzed by XRD and the standard sample was submitted to XRD as a second, final check. The differences between the ideal principal lines (100 planes) and the actual observed lines were calculated. The calculations were made for the main lines of chlorite and phlogopite in the "linde" standard as follows: for chlorite the ICDD 83-1381 standard number was used, which shows the main peak at 14.2497Å, and for phlogopite, the 85-2275 card number, which has the main line at 10.3800Å. The difference between the main line of the ICDD form and the respective value found in each analyzed pattern was calculated. These standard cards were from the PDF-2 Release 2010 database of the ICDD – International Center for Diffraction Data; the software used to read and compare the data was X´PertHighScore version 2011, from Panalytical.

In Table 1, these differences are presented. Next, the mean value found between the patterns analyzed before and after the analysis of the samples was calculated and thus the mean value of the displacements for the two important lines of the diffractogram was found. With the mean value found, the correct position of the peaks of the three samples studied was calculated.

To identify the interstratified phyllosilicates, data from Reynolds (1980) and Moore & Reynolds (1997) were used. It was based on the comparison between observed total diffractograms and model diffractograms for mixed or interstratified layers.

Table 1 - Calculation of differences between phlogopite, chlorite and linde standard lines.

Standard	ICDD File	1st.peak Å	2st.peak Å	Δ chlorite-linde I	Δ chlorite-linde II	Average
				Δ phlogopite-linde I	Δ phlogopite -linde II	
Linde I*	-	13.96896	9.95825	-	-	-
Linde II*	-	13.99352	9.95466	-	-	-
Chlorite	83-1381	14.24970	-	0.28074	0.25618	0.268460
Phlogopite	85-2275	-	10.3800	0.42175	0.42534	0.423545

* Linde I: standard analyzed before; linde II*: standard analyzed after the real sample run.

Quantitative chemical analyzes were performed by wavelength dispersion X-ray fluorescence (WDS), using 2g of each sample prepared by the fusion technique with $Li_2B_4O_7$ flux in a Claisse fusion machine. The equipment used was a PW 2404 spectrometer (Philips-PANalytical), with a rhodium anode tube.

Particles from the three samples were examined and the images obtained using a scanning electron microscope (SEM), FEI brand, model Quanta 200 FEG (field-emission gun). The chemical analyzes of microregions were performed with an energy dispersion X-ray spectrometer (EDS) Bruker brand, Esprit software.

2.2.2 Thermogravimetric analysis

Thermogravimetric analyzes were carried out up to 1000°C with a heating rate of 10°C/min, N_2 flow of 20 mL/min in an alumina crucible; the equipment used was the Shimadzu DTG-60H thermobalance.

3. Results and discussion

3.1 X-ray diffraction and quantitative chemical analysis

The results confirmed the presence of the most interesting minerals in the study: interstratified phyllosilicates, vermiculite and apatite, as shown in the following diffractograms.

The minerals identified by X-ray diffraction in the Mosaic sample (Figure 1) were vermiculite (abundant), interstratified phyllosilicate (low concentration, about 10%), apatite, diopside and dolomite (medium concentration); quartz and ilmenite (low concentration).
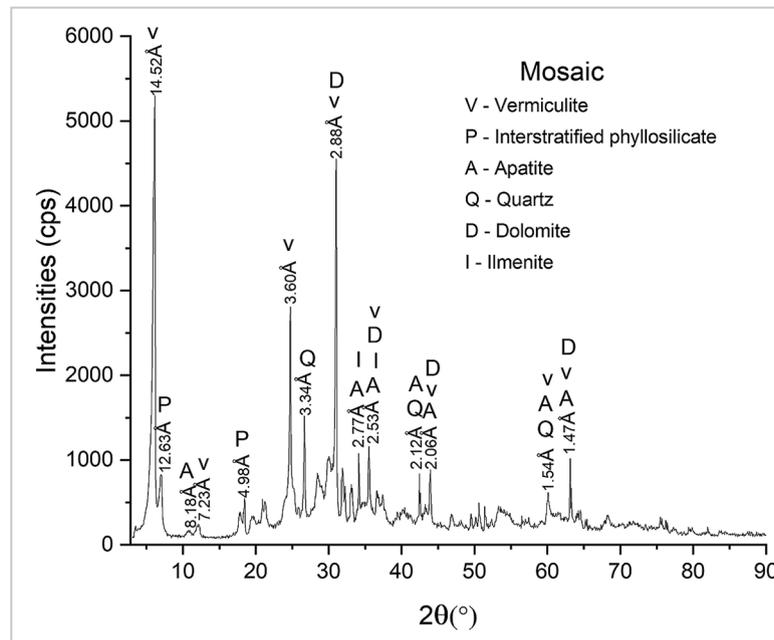

Figure 1 - X-ray diffractogram of the Mosaic sample.

In the Rocha Alterada sample, X-ray diffraction identified the following minerals (Figure 2): vermiculite (medium concentration), interstratified phyllosilicate (low concentration, about 15%), diopside (abundant), ilmenite (medium); apatite and magnetite (low concentration).
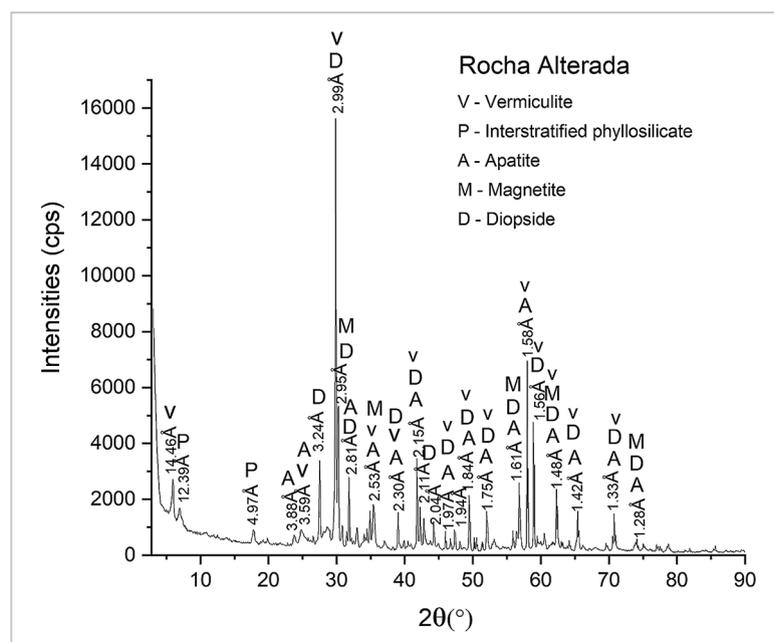

Figure 2 - X-ray diffractogram of the Rocha Alterada sample.

The minerals identified by X-ray diffraction in the Mica Base 1 sample (Figure 3) were: interstratified phyllosilicate (abundant), vermiculite (low); diopside and ilmenite (medium); apatite and magnetite (low).

The mineral compositions of the three samples are consistent with their chemical analyzes in Table 2 and with results from previous research (Chula and Brandão, 2004; Neumann *et al.*, 2011).
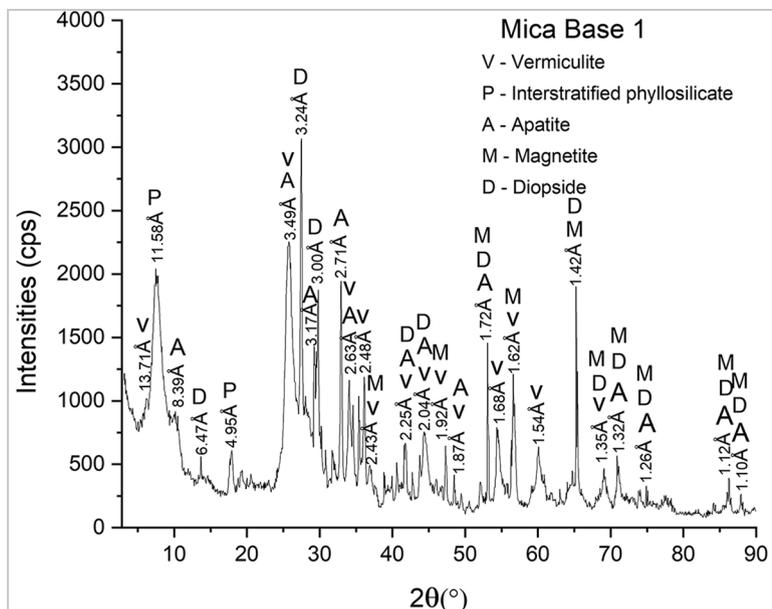

Figure 3 - X-ray diffractogram of the Mica Base 1 sample.

Table 2 - Chemical analyzes.

Composition (mass %)	Al_2O_3	CaO	Cr_2O_3	Fe_2O_3	K_2O	MgO	MnO	Na_2O	P_2O_5	SiO_2	TiO_2	ZrO_2	F	BaO	SrO	LOI (1000°C)
Mosaic	6.72	10.22	0.02	16.12	0.84	8.78	0.31	0.00	5.73	33.89	4.44	0.10	0.33	<0.01	0.15	12.25
Rocha Alt.	2.50	18.25	<0.01	16.63	0.86	11.85	0.19	0.68	3.56	36.29	5.51	0.01	0.49	<0.01	0.22	2.68
Mica Base 1	6.31	16.36	<0.01	14.93	3.56	9.61	0.21	0.29	2.09	35.68	6.19	0.27	0.38	<0.01	0.12	3.85

All samples have interstratified phyllosilicates, identified by the presence of the peaks between 11.59Å and 12.63Å in the X-ray diffractograms and in Table 3. This identification was based on the comparison between the observed complete diffractograms and the model diffractograms for mixed layers or interstratified layer phyllosilicates, according to data from Reynolds (1980) and Moore and Reynolds (1997).

Table 3 - Corrected X-ray diffraction results of the phyllosilicates.

Sample	Diagnostic peak, vermiculite (Å)	Diagnostic peak, phyllosilicate (Å)
Mosaic	14.52469	12.63467
Rocha Alterada	14.46992	12.39227
Mica Base 1	13.71376	11.58987

Table 4 shows the data from the Reynolds model (1980) and the X-ray diffraction data from the samples. According to the values presented by Reynolds (1980), it was observed that the interstratified phyllosilicates present in the samples correspond to mixed structures of the mica/vermiculite type, the layers being ordered or regular. However, the proportions of mica and vermiculite were different in the three cases, as shown in Table 4.

Table 4 - Diffraction data of the studied samples and the Reynolds model (1980).

Sample	Interstratified phyllosilicate		Reynolds		Sample	
	Mica	Vermiculite	1st.peak Å	2st.peak Å	1st.peak Å	2st.peak Å
Mosaic	40%	60%	12.6	3.49	12.63	3.44
Rocha Alterada	50%	50%	12.3	3.47	12.39	-
Mica Base 1	70%	30%	11.6	3.43	11.58	3.43

3.2 Scanning electron microscopy and EDS microanalysis

All phyllosilicates observed in SEM images have lamellar habit and exfoliation in very thin plates (Figures 4, 5 and 6). In all EDS microanalysis, these phyllosilicates showed variable compositions, but within short ranges, of the SiO_2, Al_2O_3, MgO, CaO and FeO elements (reported as oxides), in Tables 5, 6 and 7. Therefore, the K_2O content is the only microchemical parameter to distinguish the mineral species: a) when the % of K_2O is very low or tends to zero, the mineral is vermiculite (Gruner, 1934); b) when this content lies between 1.0 and 8.5%, this characterizes the mixed layer or interstratified phyllosilicate; c) the original or even slightly altered mica would have K_2O contents ranging from 9.2 to 11.8% (WebMinerals, 2017).
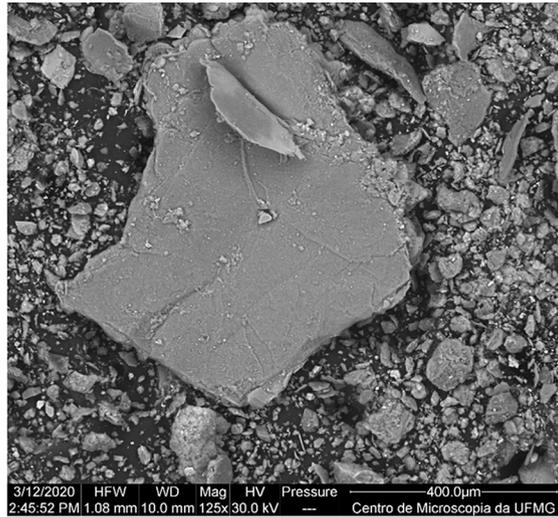

Figure 4 - Backscattered electrons image (BEI) of the Mosaic sample.

Table 5 - EDS microanalysis of the Mosaic sample in Figure 4.

Composition (%)	Al_2O_3	CaO	Fe_2O_3	K_2O	MgO	MnO	SiO_2	P_2O_5	TiO_2	Mineral
Mosaic	23.74	1.48	21.78	5.75	10.57	0.00	33.59	0.00	3.08	Interstratified phyllosilicate

EDS microanalysis (Table 5) was performed on the big particle in Figure 4, which provided high levels of silicon oxide, iron and aluminum, average content of magnesium oxide and low content of calcium and titanium. The potassium oxide content (5.75%), together with the main particle morphology characterizes an interstratified phyllosilicate.

Figure 5 shows a lamellar particle. By microanalysis (Table 6), carried out in the particle center, an interstratified phyllosilicate is identified, with a higher content of the mica component, due to the relatively high K_2O content, but still below 9.2%.
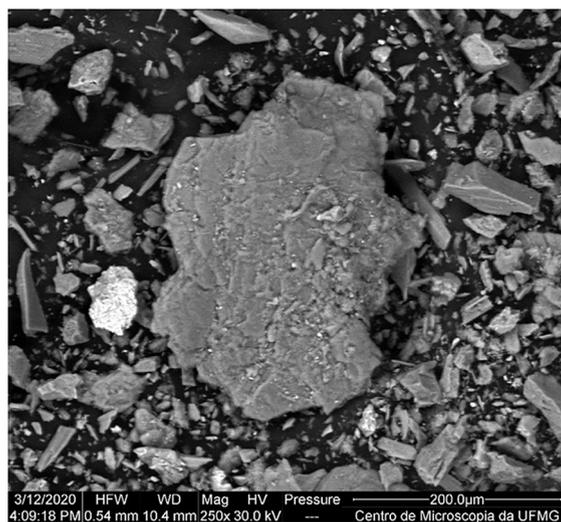

Figure 5 - Backscattered electrons image (BEI) of the Rocha Alterada sample.

Table 6 - EDS microanalysis of the Rocha Alterada sample in Figure 5.

Composition (%)	Al_2O_3	CaO	Fe_2O_3	K_2O	MgO	MnO	SiO_2	P_2O_5	TiO_2	Mineral
Rocha Alterada	18.77	1.58	21.67	7.80	16.87	0.00	30.68	0.00	2.63	Interstratified phyllosilicate

In Figure 6 there is a lamellar particle in the central part of the image. Micro-analysis (Table 7) was performed at the particle center. Thus, this is practically a biotite mica, due to the percentage of K_2O already very close to the 9.2 limit.
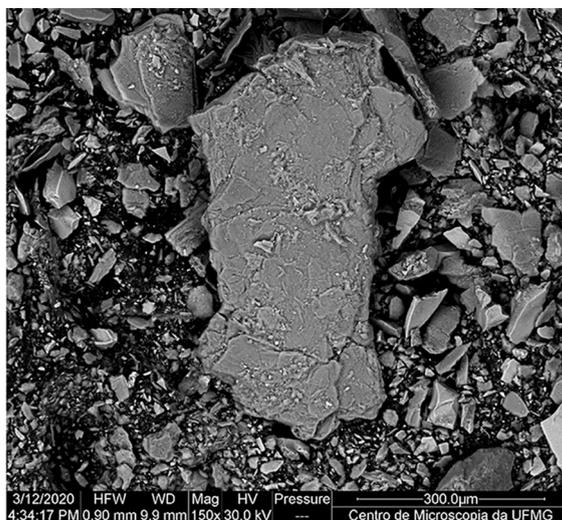

Figure 6 - Backscattered electrons image (BEI) of the Mica Base 1 sample.

Table 7 - EDS microanalysis of the Mica Base 1 sample in Figure 6.

Composition (%)	Al_2O_3	CaO	Fe_2O_3	K_2O	MgO	MnO	SiO_2	P_2O_5	TiO_2	Mineral
Mica Base 1	16.85	0.85	29.79	9.06	11.71	0.18	29.51	0.00	2.05	Mica

3.3 Thermogravimetric analysis

The thermogravimetry (TG) results of the Mosaic sample are shown in Figure 7 and Table 8. The temperature and mass loss data are consistent with the composition of minerals that undergo pyrolysis in the studied temperature range (Speyer, 1993; Földvári, 2011). In this sample, these minerals were vermiculite, interstratified phyllosilicate and dolomite.
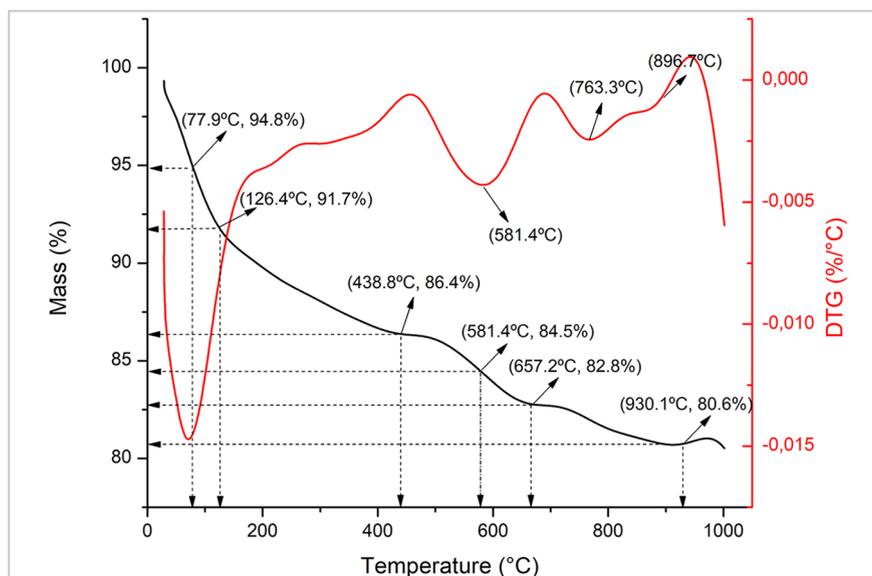

Figure 7 - Thermogravimetric analysis of the Mosaic sample.

Table 8 - Thermogravimetry of the Mosaic sample.

Assignment	Initial temperature °C	Final temperature °C	Mass loss %
Moisture	25	100-126	8.3
Vermiculite H_2O	126	439	5.3
Interstratified H_2O	500	657	3.6
Dolomite CO_2	700	897	2.2

Total mass loss: 19.4%.

Figure 8 and Table 9 show the thermogravimetric analysis of the Rocha Alterada sample. The minerals that undergo pyrolysis are interstratified phyllosilicate and vermiculite.
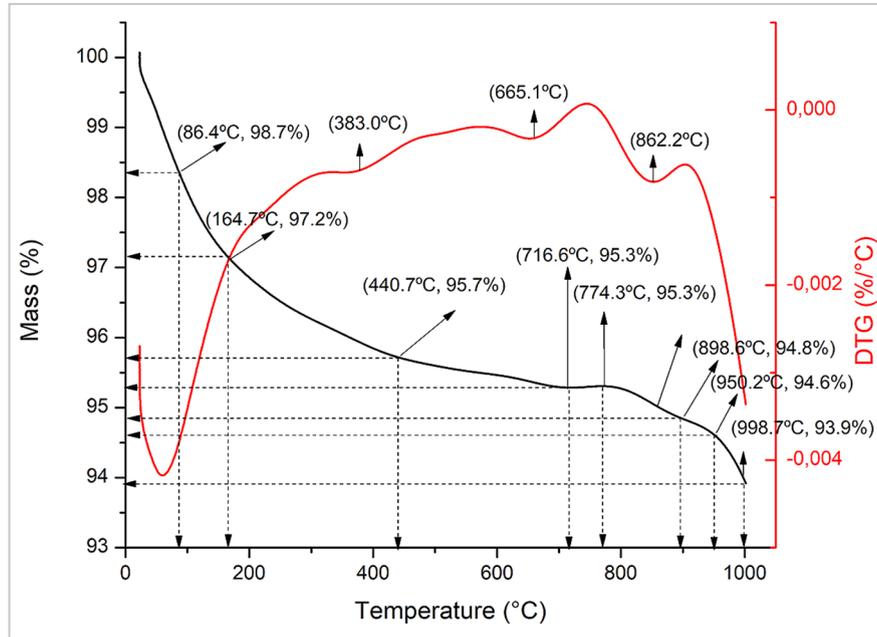

Figure 8 - Thermogravimetric analysis of the Rocha Alterada sample.

Table 9 - Thermogravimetry of the Rocha Alterada sample.

Assignment	Initial temperature °C	Final temperature °C	Mass loss %
Moisture	25	100	1.5
Vermiculite H_2O	100	717	3.2
Interstratified H_2O	774	950	0.7
Interstratified H_2O	950	999	0.7

Total mass loss: 6.1%.

The thermogravimetric data of the Mica Base 1 sample, shown in Figure 9 and Table 10, demonstrate that, also here, interstratified phyllosilicate and vermiculite are the ones that lose mass, like H_2O.
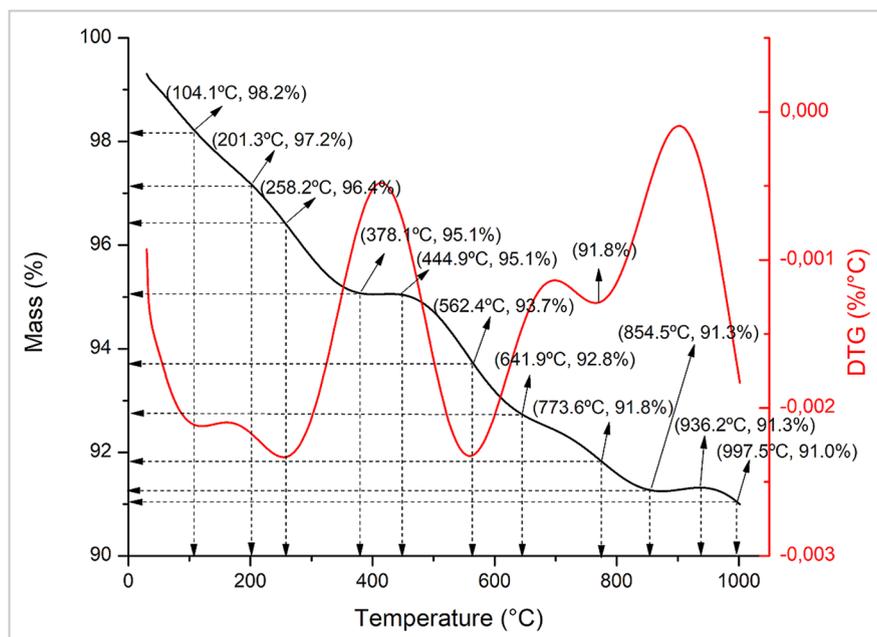

Figure 9 - Thermogravimetric analysis of the Mica Base 1 sample.

Table 10 - Thermogravimetry of the Mica Base 1 sample.

Assignment	Initial temperature °C	Final temperature °C	Mass loss %
Moisture	25	104	1.8
Vermiculite H_2O	104	378	3.1
Interstratified H_2O	445	855	3.8
Interstratified H_2O	936	997	0.3

Total mass loss: 9.0%.

The thermogravimetry results are consistent with the data collected in the other analyses. In the case of the Mica Base 1 sample, which has the highest interstratified phyllosilicate content, thermogravimetry showed the highest relative mass loss, with 4.1%, compared to the vermiculite loss, which was 3.1%.

In two samples, two ranges were observed at the highest temperatures, where there was mass loss. Both are attributed to the interstratified phyllosilicate, as follows: in the lower range, the pyrolysis would be of the H_2O from the vermiculite layers, and in the higher range, the loss would be due to the hydroxyls of the mica layers.

4. Conclusions

Quantitative chemical, XRD, TG and SEM/EDS analyzes indicated the mineralogical compositions for the studied samples. Detailed analysis by XRD allowed to determine the specific unity cell stratification, that is, the stacking sequence of the mica and vermiculite layers, in the 3 types of mixed layer phyllosilicates identified in the samples, which were always ordered (regular), according to the model by Reynolds (1980). The results are:

Mosaic: apatite, dolomite, ilmenite, quartz, vermiculite, interstratified phyllosilicate, this one with 40% mica and 60% vermiculite;

Rocha Alterada: apatite, diopside, ilmenite, magnetite, vermiculite, interstratified phyllosilicate, with 50% mica and 50% vermiculite;

Mica Base 1: apatite, diopside, magnetite, vermiculite, interstratified phyllosilicate, this one with 70% mica and 30% vermiculite.

Potassium content, reported as K_2O, is the only microchemical parameter to distinguish the phyllosilicate in EDS microanalyses. a) when the % of K_2O is very low or tends to zero, it is vermiculite; b) when this content is between 1.0 and 8.5%, this characterizes the mixed layer or interstratified phyllosilicate; c) the original or even slightly altered mica would have K_2O contents ranging from 9.2 to 11.8%.

The improved knowledge of the mineralogical composition of these complex ores can contribute to better explain problems encountered in their concentration. The micaceous minerals which are a great part of this problem and are now better known, including the fact that fresh mica (biotite) is very rare. The weathered products are the dominant phyllosilicates: vermiculite and interstratified species.

References

ALBUQUERQUE, R. O.; PERES, A. E. C.; AQUINO, J. A.; PRAES, P. E.; PEREIRA, C. A. Pilot scale direct flotation of a phosphate ore with silicate-carbonate gangue. *Procedia Engineering,* v. 46, p. 105–110, 2012. DOI: doi.org/10.1016/j.proeng.2012.09.452.

ASSIS, S. M.; BRANDÃO, P. R. G.; LEAL FILHO, L. S.; COELHO, E. M. The influence of micas and related minerals on the direct anionic flotation of apatite from the Tapira mine, Brazil–Part2. Studies on apatite/micaceous minerals mixtures. *In*: ZHANG, P.; SWAGER, K.; LEAL FILHO, L. S.; EL-SHALL, H. (ed.). *Beneficiation of phosphates*: technology advance and adoption. Littleton: Society for Mining, Metallurgy, and Exploration (SME), 2010. p.369-377. ISBN 978-0-87335-319-9.

AZZONE, R. G.; RUBERTI, E. Evolução composicional dos filossilicatos no perfil intempérico do complexo ultramáfico alcalino-carbonatítico de Catalão I (GO). *Geologia USP - Série Científica,* v.10, n. 2, p. 23-43, 2010.

BAILEY, S. W.; BANFIELD, J. F.; BARKER, W. W; KATCHAN, G. Dozyite, a 1:1 regular interstratification of serpentine and chlorite. *American Mineralogist,* v. 80, n. 1-2, p. 65-77, 1995.

BIAN, Z; KAWI, S. Preparation, characterization and catalytic application of phyllosilicate: a review. *Catalysis Today,* v. 339, p. 3-23, 2020. DOI: doi.org/10.1016/j.cattod.2018.12.030.

CHULA, A. M. D.; BRANDÃO, P. R. G.; AQUINO, J. A. Caracterização de minérios fosfáticos com elevados teores de carbonatos e silicatos da mina de Tapira-MG. *In*: ENCONTRO NACIONAL DE TRATAMENTO DE MINÉRIOS E METALURGIA EXTRATIVA, 20., 2004, Florianópolis, SC. *Anais [...]*. [*S. l.*]: ENTMME,

2004. v. 1, p.17-24.

ESCAMILLA-ROA, E.; HERNÁNDEZ-LAGUNA, A.; SAINZ-DÍAZ, C. I. Cation arrangement in the octahedral and tetrahedral sheets of cis-vacant polymorph of dioctahedral 2:1 phyllosilicates by quantum mechanical calculations. *American Mineralogist,* v. 98, n. 4, p. 724-735, 2013.

FÖLDVÁRI, M. *Handbook of thermogravimetric system of minerals and its use in geological practice.* Budapest: Geological Institute of Hungary, 2011. 180 p.

GRUNER, J. W. The structures of vermiculites and their collapse by dehydration. *American Mineralogist,* v. 19, n. 12, p. 557-575, 1934.

HILLIER, S. Origin, diagenesis, and mineralogy of chlorite minerals in Devonian Lacustrine Mudrocks, Orcadian Basin, Scotland. *Clays and Clay Minerals,* v. 41, p. 240-259, 1993.

LIU, X.; RUAN, Y.; LI, C.; CHENG, R. Effect and mechanism of phosphoric acid in the apatite / dolomite flotation system. *International Journal of Mineral Processing,* v. 167, p. 95–102, 2017. DOI 10.1016/j.minpro.2017.08.006.

MOORE, D. M.; REYNOLDS, R. C. *X-ray diffraction and the identification and analysis of clay minerals.* 2nd. ed. New York: Oxford University Press, 1997.

NADEAU, P. H.; WILSON, M. J.; MCHARDY, W. J.; TAIT, J. M. Interstratified clays as fundamental particles. *Science,* v. 225, n. 4665, p. 923–925, 1984.

NEUMANN, R.; COSTA, G. E. L.; GASPAR, J. C.; PALMIERI, M.; SILVA, E. S. The mineral phase quantification of vermiculite and interstratified clay minerals-containing ores by X-ray diffraction and Rietveld method after K cation Exchange. *Minerals Engineering,* v.24, n.12, p.1323-34, Oct. 2011. DOI: doi.org/10.1016/j.mineng.2011.05.017.

PLANÇON, A. Diffraction by layer structures containing different kinds of layers and stacking faults. *Journal of Applied Crystallography,* v. 14, p. 300–304, 1981. DOI 0021-8898/81/050300-05.

REYNOLDS, R. C. Interstratified clay minerals. In: BRINDLEY, G.W.; BROWN, G. (ed.). *Crystal structures of clay minerals and their X-ray identification.* London: Mineralogical Society of Great Britain and Ireland, 1980. p. 249–304.

SCHREYER, W.; MEDENBACH, O.; ABRAHAM, K.; GEBERT, W.; MULLER, W. F. Kulkeite, a new metamorphic phyllosilicate mineral: ordered 1:1 chlorite / talc mixed-layer. *Contributions to Mineralogy and Petrology,* v. 80, n. 2, p. 103-109, 1982.

SIS, H.; CHANDER, S. Reagents used in the flotation of phosphate ores: a critical review. *Minerals Engineering,* v. 16, n. 7, p. 577–85, 2003. DOI 10.1016/S0892-6875(03)00131-6.

SPEYER, R. F. *Thermal analysis of materials.* Boca Raton: CRC Taylor & Francis, 1993. 285 p.

VEBLEN, D. R.; GUTHRIE, G. D.; LIVI, K. J. T. High-resolution transmission electron microscopy and electron diffraction of mixed-layer illite/smectite: experimental results. *Clays and Clay Minerals,* v. 38, n. 1, p. 1–13, 1990.

WANG, L.; XU, H. Geochemical chaos: periodic and nonperiodic growth of mixed-layer phyllosilicates. *Geochimica et Cosmochimica Acta,* v. 70, n. 8, p. 1995–2005, 2006. DOI 10.1016/j.gca.2006.01.002.

WEBMINERALS. [*S. l.: s. n.*], 2017. Available at: http://webmineral.com/. Accessed: 14 Jun 2017.

XU, H.; VEBLEN, D. R. Interstratification and other reaction microstructutures in the chlorite-berthierine series. *Contributions to Mineralogy and Petrology,* v. 124, p. 291-301, 1996.

XU, H.; ZHANG, Y.; VEBLEN, D. R. Periodic and nonperiodic interstratification in the chlorite-biotite series. *American Mineralogist,* v. 81, p. 1396-1404, 1996.